Japanese Journal of Veterinary Research 71(1): 20-26, 2023

JJVR

SHORT COMMUNICATION Clinical Case Report

Computed tomography and magnetic resonance imaging findings with left adrenal pheochromocytoma infiltrating the spinal canal and liver metastases in a dog

Shinya Mizutani[1,†)], Yuko Mizutani[2,†)], Hiroyuki Satoh[3,*)], Yoshimichi Goda[3)], Taketoshi Asanuma[1)] and Shidow Torisu[4)]

[1)] Clinical Veterinary Medicine, Department of Veterinary Medicine, Faculty of Veterinary Medicine, Okayama University of Science Imabari campus, 1-3 Ikoinooka, Imabari City, Ehime 794-8555, Japan.
[2)] University of Miyazaki Veterinary Teaching Hospital, 1-1 Gakuen Kibana-dai Nishi, Miyazaki City, Miyazaki 889-2192, Japan.
[3)] Laboratory of Veterinary Clinical Radiology, Department of Veterinary Sciences, Faculty of Agriculture, University of Miyazaki, Miyazaki 889-2192, Japan.
[4)] Companion Animal Surgery, Department of Veterinary Medicine, Rakuno Gakuen University, 582, Bunkyodai-Midorimachi, Ebetsu, Hokkaido 069-8501, Japan

Received for publication, February 7, 2022; accepted, December 16, 2022

Abstract

Recently, detection of canine primary adrenal mass has increased owing to progress in diagnostic imaging. Adrenocortical adenoma, adrenocortical carcinoma, and pheochromocytoma are representative primary adrenal masses; the latter two may invade intravascularly and metastasize to other organs. We encountered a dog exhibiting progressive hindlimb paraplegia. Multimodal imaging including computed tomography (CT) and magnetic resonance imaging (MRI) revealed that the cause of the paraplegia was infiltration of a left adrenal pheochromocytoma into the spinal canal. In addition, MRI detected small liver metastatic lesions that were not detected by CT.

Key Words: Dogs, Pheochromocytoma, Spinal canal

Canine primary adrenal tumors account for 1%–2% of all canine tumors[12)], which makes them relatively rare. Representative examples of adrenal tumors include adrenocortical adenoma, adrenocortical carcinoma, and pheochromocytoma. Pheochromocytoma is a type of neuroendocrine tumor derived from the chromaffin cells of the adrenal medulla that can produce catecholamines. Dogs with pheochromocytomas generally have varied clinical symptoms related to catecholamine secretion such as sudden collapse, exercise intolerance, anorexia, and hypertension[5)], although they are sometimes asymptomatic. Up to 40% of canine pheochromocytomas have been reported to metastasize to distant organs and lymph nodes and are reported to cause vascular invasion in 35%–82% of cases[1,5,8)]. Although there are few specific tests for diagnosing pheochromocytoma,

* Corresponding author: Hiroyuki Satoh, D.V.M., Ph.D.
Laboratory of Veterinary Clinical Radiology, Department of Veterinary Sciences, Faculty of Agriculture, University of Miyazaki, Miyazaki 889-2192, Japan.
Phone: +81-985-58-7286
E-mail: hsatoh@cc.miyazaki-u.ac.jp
† These authors contributed equally to this work.
doi: 10.57494/jjvr.71.1_20

the measurement of metanephrine and normetanephrine concentrations in the plasma and urine has been reported to be effective[6,15].

Computed tomography (CT) of the adrenal tumors can obtain information including the detection of an adrenal tumor, formation of a tumor plug in the surrounding vascular system, presence or absence of calcification, and detection of distant metastases. Moreover, in recent years, studies have reported the use of triple-phase CT to classify primary adrenal masses, and their effectiveness is apparent[18]. On the contrary, reports of magnetic resonance imaging (MRI) of the adrenal glands of dogs are limited, but they have increased in recent years[7,10,11]. Although a report showed MRI can detect spinal cord metastasis of pheochromocytoma in a dog[17], few reports have recorded the effectiveness of abdominal MRI. In this study, we report a canine case of pheochromocytoma infiltrating the spinal canal detected by CT and MRI and include new findings regarding liver metastasis.

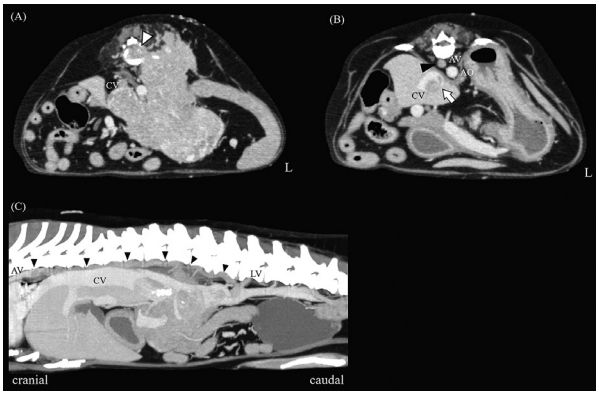

Fig. 1. Computed tomography images
A. Transverse section (venous phase)
B. Transverse section (venous phase)
C. Sagittal section (maximum intensity projection)
The left adrenal mass in this figure was from the venous phase. The mass was suspected to infiltrate the spinal canal at the L1–2 intervertebral space (white arrowhead) (A) and was shown infiltrating the caudal vena cava (white arrow line) (B). The mass also infiltrated the azygos vein from the lumbar vein (black arrowhead) (B, C).
AO, abdominal aorta; AV, azygos vein; CV: caudal vena cava; LV, lumbar vein

An 11-year-old castrated male, miniature Dachshund (8.5 kg body weight) was presented at a veterinary clinic with progressive symptoms of paraparesis to paraplegia that had started about 2 weeks ago. The referring veterinarian suspected intervertebral disk herniation as the cause of the paraparesis, but response to medical treatment was poor and symptoms progressed. General condition was unremarkable on the first visit to our veterinary hospital (day 1); body temperature, 38.0˚C; heart rate, 148 beats per minute; respiratory rate, 60 beats per minute; systolic arterial blood pressure, 174 mmHg; mean arterial blood pressure, 121 mmHg; and diastolic arterial blood pressure, 81 mmHg. Blood tests showed no major abnormalities. Neurological examination revealed the disappearance of posture responses in both hind limbs and hyperreflexia of the patellar tendon reflex. Based on these findings, we suspected spinal disorders in the third thoracic (T3) region to the third lumbar (L3) region.

An abdominal radiograph revealed a large mass lesion on the left dorsal side of the abdominal cavity and cranial side of the left kidney. Ultrasonography showed a mass of 50–60 mm in size in the same area as detected by radiography. Continuity between the mass and liver, spleen, and right and left kidneys was not observed. An embolus was also found in the caudal vena cava. Although a tumor plug was suspected, finding the continuity between the embolus and the mass was difficult. CT and MRI were performed under general anesthesia, during which no significant changes in the blood pressure occur. For CT, a 16-slice multidetector helical CT scanner (Aquilion LB; Canon Medical Systems Co., Otawara, Japan) was used. After pre-contrast imaging (before the injection of a contrast medium), iohexol (600 mgI/kg) was injected for 20 s into the cephalic vein, and a triple-phase contrast-enhanced CT was performed. CT images were analyzed using the image analysis software AZE Arata (AZE Corporation, Tokyo, Japan). The CT findings suggested that the abdominal mass was a massive tumor arising from the left adrenal gland (Fig. 1A). The embolus in the caudal vena cava was confirmed as a tumor plug because it was a continuous mass (Fig. 1B). The tumor appeared to infiltrate into the caudal vena cava from slightly cranial to the left renal vein. The range of the

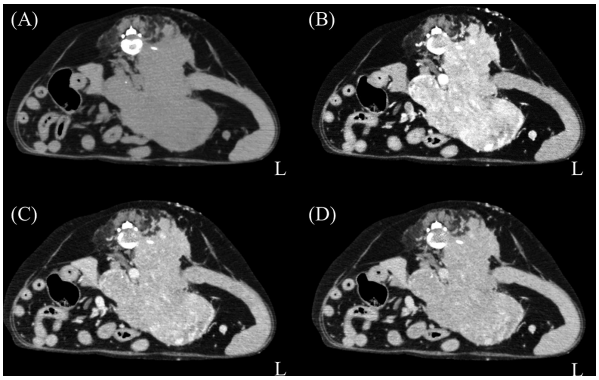

Fig. 2. Triple-phase computed tomography (transverse section)
A. Pre-contrast
B. Arterial phase
C. Venous phase
D. Equilibrium phase
Pre-contrast (A), arterial phase (B), venous phase (C), and equilibrium phase (D) were compared at the same site of the left adrenal tumor. Contrast enhancement was strong in the arterial phase and was attenuated in the venous and equilibrium phases. This finding was suspected as pheochromocytoma.

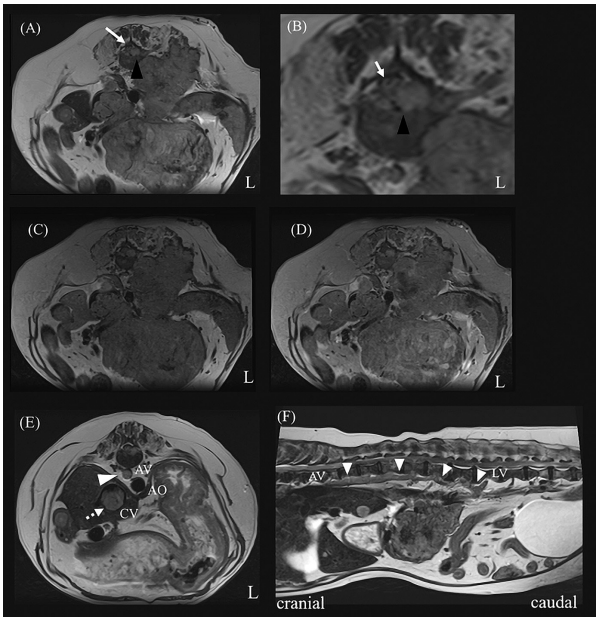

Fig. 3. Magnetic resonance imaging
A. Transverse section (T2WI)
B. Transverse section (T2WI, enlarged view)
C. Transverse section (T1WI)
D. Transverse section (contrast-enhanced T1WI (CET1WI))
E. Transverse section (T2WI)
F. Sagittal section (T2WI)
The left adrenal mass showed more hyperintensity and some hypointensity in T2WI (A). The tumor (black arrowhead) was observed on the left ventral side of the L1–2 spinal canal, and the spinal cord (white arrow line) was squeezed to the right dorsal side by the tumor (A, B). On T1WI, the left adrenal tumor and tumor infiltrating the spinal canal showed hypointensity to isointensity compared with the skeletal muscles (C). On CET1WI, most of the left adrenal tumor showed hyperintensity, and the tumor infiltrating the spinal canal showed slight hyperintensity (D). The tumor plugs infiltrated the azygos vein (white arrowhead) and caudal vena cava (white dotted line) (E). The tumor plugs in the azygos vein infiltrated from the lumbar vein (white arrowhead) (F).
AO, abdominal aorta; AV, azygos vein; CV, caudal vena cava; LV, lumbar vein; T2WI, T2-weighted imaging; T1W1, T1-weighted imaging

tumor plug within the caudal vena cava was from slightly cranial to the hepatic vein of the caudate lobe to near the caudal end of the right kidney. In addition, tumor plugs were observed continuously in the azygos vein from the caudal vena cava via the lumbar vein at the L3–4 region (Fig. 1B, C). The mass appeared to grow out of the abdominal cavity through the renal fascia and invade the muscle tissue of the dorsal lumbar area. There was a suspicious finding of invasion into the spinal canal from between the first and second lumbar (L1–2) vertebrae (Fig. 1A). In the triple-phase CT, the left adrenal mass showed the strongest contrast enhancement effect in the arterial phase, and this decreased in the venous phase and equilibrium phase as time proceeded (Fig. 2A–D). As with other findings, multiple nodular lesions showing the strongest contrast-enhancing effect in the arterial phase were observed in the caudate lobe and left lateral lobe of the liver. MRI was performed for a detailed examination of the vertebral or intervertebral canal lesions observed by CT and evaluation of adrenal tumors and nodular lesions of the liver.

For MRI, a 3.0 Tesla MRI scanner (Vantage Titan 3T; Canon Medical Systems Co., Otawara, Japan) was used. A gadolinium-based contrast medium (0.1 mmol/kg) bolus injection was made into the cephalic vein. MRI showed that the left adrenal tumor had predominant hyperintensity and some hypointensity in the T2-weighted image (T2WI) (Fig. 3A, B). Moreover, MRI more clearly showed that a part of the tumor compressed the spinal cord from the ventral left side at the L1–2 level (Fig. 3B). On T1-weighted image (T1WI), the left adrenal tumor and tumor infiltrating the spinal canal showed hypointensity to isointensity

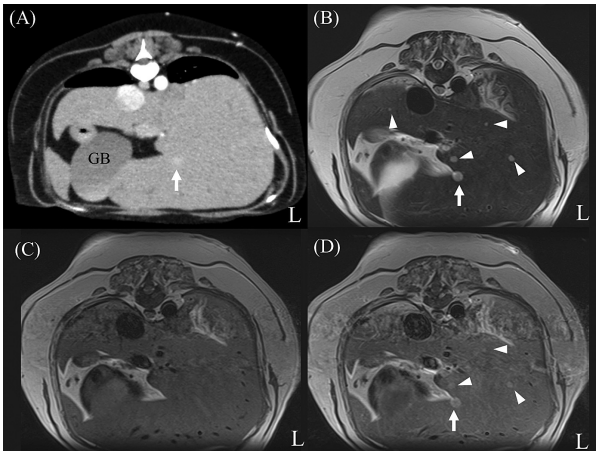

Fig. 4. Comparison of CT and MRI in liver nodular lesions (transverse section)
A. Arterial phase in CT
B. T2WI in MRI
C. T1WI in MRI
D. Contrast-enhanced T1WI (CET1WI) in MRI
The arterial phase in CT confirmed one nodular lesion (white arrow line) in the liver parenchyma (A). T2WI and CET1WI confirmed the same one nodular lesion (white arrow line) in CT (B, D). In addition, T2WI and CET1WI confirmed more nodular lesions (white arrowhead) than CT (B, D). The liver nodular lesion (white arrow line) was the same lesion in CT, T2WI, and CET1WI. T1WI did not confirm liver nodular lesions (C).
GB, gall bladder; MRI, magnetic resonance imaging; T2WI, T2-weighted imaging; T1W1, T1-weighted imaging

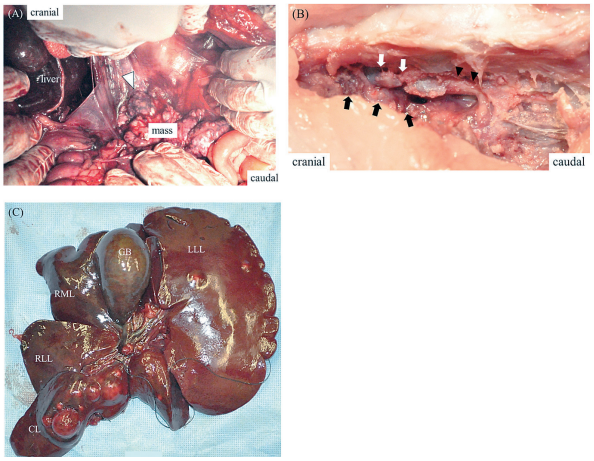

Fig. 5. Necropsy
A. Exit site of the tumor out of the abdominal cavity
B. Spinal cord (L1–2)
C. Nodular lesions in liver parenchyma
As was observed in CT and MRI, the tumor infiltrated outside the abdominal cavity from the point of the white arrowhead (A). The infiltration of the tumor into the spinal canal (black arrow line) was confirmed around the L1–2 spinal cord (black arrowhead) (B). A part of the spinal cord was confirmed necrotic (white arrow line). Many nodular lesions were confirmed in the liver parenchyma (C).
CL, caudate lobe; CV, caudal vena cava; GB, gall bladder; LLL, left lateral lobe; RML, right medial lobe; RLL, right lateral lobe

compared with the skeletal muscles (Fig. 3C) and was enhanced with gadolinium on T1WI (Fig. 3D). The MR appearance of the tumor plugs was highly suggestive of infiltration in the veins (Fig. 3E, F). In the liver parenchyma, several nodular lesions that were not shown on CT, including other liver lobes, can be confirmed on MRI (Fig. 4A, B). These showed hyperintensity on T2WI and isointensity on T1WI and were enhanced with gadolinium on T1WI (Fig. 4B, C, D).

From the results of multimodal imaging tests in this case, the progressive paraparesis was thought to be caused by spinal cord compression following the infiltration of the left adrenal gland tumor into the spinal canal. Radical surgical treatment was rejected based on these multimodal imaging findings, with suspicion of invasion of the tumor into the blood vessels and liver nodular lesions that were suspected metastases. On day 41, the patient died at home of sudden cardiopulmonary arrest. We performed a necropsy after obtaining the owner's consent. At necropsy, a large tumor (86 × 87 × 67 mm; same size in CT) was identified in the abdominal cavity, similar to the CT and MRI findings, and a site infiltrating outside the abdominal cavity was confirmed (Fig. 5A). Neoplastic lesions were noted around the spinal cord at L1–2 (Fig. 5B). Multiple nodular lesions were present in the liver parenchyma (Fig. 5C). The left adrenal tumor, tumor plugs, and soft tissue around the spine (L1–2) and within the spinal canal and liver were all diagnosed as pheochromocytomas following histopathological examination (Fig. 6A–D).

We encountered a canine case with progressive paraparesis/paraplegia caused by spinal canal infiltration of a pheochromocytoma. To date, only one report has focused on the infiltration of pheochromocytomas into the spinal canal that included two cases[13]. These previous two cases were examined at a veterinary hospital with the

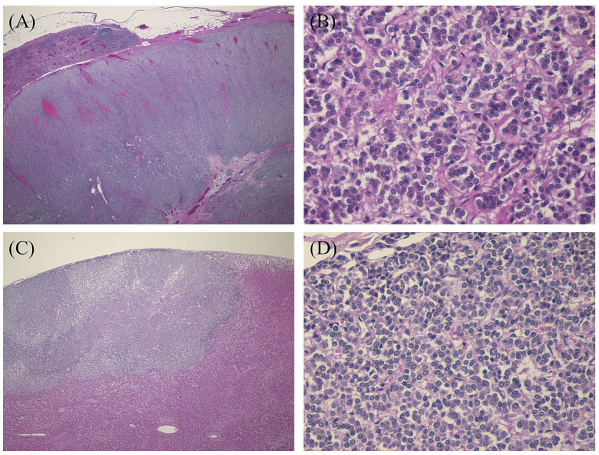

Fig. 6. Histopathology
A. Left adrenal gland (low-power field)
B. Left adrenal gland (high-power field)
C. Liver lesion (low-power field)
D. Liver lesion (high-power field)
The left adrenal tumor and liver nodular lesion were diagnosed as pheochromocytoma.
(Hematoxylin and eosin staining: (A, C) 10×, (B, D) 400×

main complaint of paraparesis, and both clinical courses were progressive, similar to the current case. The previous two cases were euthanized because they exhibited dorsal lumbar pain, and infiltration of the pheochromocytoma into the spinal canal was confirmed by necropsy in these both cases. In one of these cases, metastatic tumor masses were found in the spinal canal at C1–3 (cervical) and L1–6 levels and systemically through the body. In one case of this previous report, the pheochromocytoma had infiltrated into the spinal canal from between L1 and L2 as in the current case. In this previous report, the pheochromocytomas had infiltrated into the spinal canal from between L1–2 and T13–L5. The present case and previous two cases may have infiltrated into the spinal canal from similar thoracolumbar regions. In addition, the vascular invasion of canine adrenal masses occurred via the veins[16]. Therefore, these spinal canal infiltrations of pheochromocytomas were suggested to have occurred via the veins. In canine anatomy[2], the left adrenal vein joins a common trunk of the left cranial abdominal vein and the left caudal phrenic vein that flows into the caudal vena cava. In addition, the left cranial abdominal vein joins the hemiazygos vein. The hemiazygos vein joins the lumbar veins that join the intervertebral veins. Therefore, we suggested that the route of the spinal canal infiltration of pheochromocytoma was the intervertebral vein via the hemiazygos vein.

According to a previous report examining the differentiation of adrenal tumors using triple-phase CT[18], pheochromocytoma shows its strongest contrast enhancement pattern in the arterial phase, and this decreases in the venous and equilibrium phases as time proceeds. Our pheochromocytoma of the left adrenal gland showed a similar contrast enhancement on the triple-phase CT. In addition, intravascular and vertebral canal tumors and nodular lesions in the caudate lobe of the liver all showed the same contrast pattern. Therefore, we considered that these findings were related to the lesions from the pheochromocytoma of the left adrenal gland.

In this case, the pheochromocytoma of the left adrenal gland in the abdominal cavity showed a mixed of hyperintensity and hypointensity regions on T2WI. These findings were consistent with a previous report that showed the pheochromocytoma of the left adrenal gland in a dog on T2WI by MRI[17]. Since pheochromocytoma is accompanied by fibrosis, necrosis, calcification, or hemorrhage, MRI in humans has revealed various findings[3,4,14]. Necrosis and hemorrhage were also confirmed in the pathological tissue of the left adrenal gland in this case, which was considered to support the current T2WI findings. In this case, both the T1WI and CET1WI of the pheochromocytoma in the left adrenal gland and spinal canal showed similar findings to T1WI and CET1WI of the human pheochromocytoma[4].

In addition, the liver findings on MRI revealed finer metastatic lesions that could not be detected by CT. MRI has high contrast resolution than CT, and it was considered that smaller metastatic lesions that could not be detected by contrast-enhanced CT could be confirmed by MRI. However, in this case, we used 3T MRI as it is a high-field MRI. It was unclear whether similar nodular lesions could be detected by low-field MRI, and this should be investigated in the future. In previously reported human cases, MRI was

superior to CT in detecting small liver metastatic lesions of ≤ 10 mm[9]. The liver metastatic lesions detected in the current case were a minimum of 5.0 mm on CT and a minimum of 1.2 mm on MRI; therefore, MRI was more successful in detecting metastatic lesions than CT. Consequently, we suggest that MRI was more sensitive than CT in detecting liver metastatic lesions in dogs, as also in humans. These findings suggest that abdominal MRI may be effective in detecting metastatic lesions in other intra-abdominal organs.

This report included only one case; thus, collecting a greater number of such cases is important to determine whether this imaging finding is applicable to all pheochromocytoma cases. Despite the above-mentioned limitation, this report is valuable, as it captured the continuity of the pheochromocytoma that infiltrated extra-abdominally and invaded the spinal canal, and we confirmed a greater number of small metastases by MRI.

References

1) Adin CA, Nelson RW. Adrenal glands. In: Veterinary surgery: small animal. Tobias KM, Johnson SA. eds. Elsevier Saunders, St. Louis. pp. 2033–2042, 2012.
2) Bezuidenhout AJ. Veins. In: Miller's anatomy of the dog, 4th ed. Evans HE, de Lahunta A, eds. Saunders/Elsevier, St. Louis. pp. 505–534, 2013.
3) Blake MA, Kalra MK, Maher MM, Sahani DV, Sweeney AT, Mueller PR, Hahn PF, Boland GW. Pheochromocytoma: an imaging chameleon. Radiographics 24, S87–S99, 2004.
4) Elsayes KM, Menias CO, Siegel CL, Narra VR, Kanaan Y, Hussain HK. Magnetic resonance characterization of pheochromocytomas in the abdomen and pelvis: imaging findings in 18 surgically proven cases. J Comput Assist Tomogr. 34, 548–553, 2010.
5) Fernandez Y, Seth M, Murgia D. Adrenal neoplasia in dogs: clinical and surgical approach. Companion Animal 20, 40–45, 2015.
6) Gostelow R, Bridger N, Syme HM. Plasma-free metanephrine and free normetanephrine measurement for the diagnosis of pheochromocytoma in dogs. J Vet Intern Med 27, 83–90, 2013.
7) Gregor KM, Knebel A, Haverkamp AK, Baumgärtner W, Volk H. Metastatic canine phaeochromocytoma with unusual manifestation. J Comp Pathol 192, 33–40, 2022.
8) Herrera MA, Mehl ML, Kass PH, Pascoe PJ, Feldman EC, Nelson RW. Predictive factors and the effect of phenoxybenzamine on outcome in dogs undergoing adrenalectomy for pheochromocytoma. J Vet Intern Med 22, 1333–1339, 2008.
9) Kulemann V, Schima W, Tamandl D, Kaczirek K, Gruenberger T, Wrba F, Weber M, Ba-Ssalamah A. Preoperative detection of colorectal liver metastases in fatty liver: MDCT or MRI? Eur J Radiol 79, e1–e6, 2011.
10) Larson RN, Schmiedt CW, Wang A, Lawrence J, Howerth EW, Holmes SP, Grey SW. Adrenal gland function in a dog following unilateral complete adrenalectomy and contralateral partial adrenalectomy. J Am Vet Med Assoc 242, 1398–1404, 2013.
11) Lee E, Choi BK, Lee SK, Choi J. 3.0-Tesla MRI of normal canine adrenal glands. Vet Radiol Ultrasoud 63, 206–215, 2022.
12) Lunn KF, Page RL. Tumors of the endocrine system. In: Withrow and MacEwen's small animal clinical oncology, 5th ed. Withrow SJ, Vail DM, Page RL. eds. Elsevier Saunders, St. Louis. pp. 504–531, 2013.
13) Platt SR, Sheppard BJ, Graham J, Uhl EW, Meeks J, Clemmons RM. Pheochromocytoma in the vertebral canal of two dogs. J Am Anim Hosp Assoc 34, 365–371, 1998.
14) Qiao HS, Feng XL, Yong L, Yong Z, Lian ZJ, Ling LB. The MRI of extraadrenal pheochromocytoma in the abdominal cavity. Eur J Radiol 62, 335–341, 2007.
15) Quante S, Boretti FS, Kook PH, Mueller C, Schellenberg S, Zini E, Sieber-Ruckstuhl N, Reusch CE. Urinary catecholamine and metanephrine to creatinine ratios in dogs with hyperadrenocorticism or pheochromocytoma,

and in healthy dogs. J Vet Intern Med 24, 1093–1097, 2010.
16) Schultz RM, Wisner ER, Johnson EG, MacLeod JS. Contrast-enhanced computed tomography as a preoperative indicator of vascular invasion from adrenal masses in dogs. Vet Radiol Ultrasound 50, 625–629, 2009.
17) Spall B, Chen AV, Tucker RL, Lahmers KK, Righter DJ, Hayles J. Imaging diagnosis-metastatic adrenal pheochromocytoma in a dog. Vet Radiol Ultrasound 52, 534–537, 2011.
18) Yoshida O, Kutara K, Seki M, Ishigaki K, Teshima K, Ishikawa C, Iida G, Edamura K, Kagawa Y, Asano K. Preoperative differential diagnosis of canine adrenal tumors using triple-phase helical computed tomography. Vet Surg 45,427–435, 2016.